

AD-A046 561

ARMY ELECTRONICS COMMAND FORT MONMOUTH N J
GROWTH AND SPECTRAL ANALYSIS OF CERIUM MAGNESIUM ALUMINATE. (U)
OCT 77 R O SAVAGE, G DE LHERY, T R AUCOIN

F/6 20/10

UNCLASSIFIED

ECOM-4540

NL

| OF |
AD
A046561



END
DATE
FILED
12-74
DDC



12

2

Research and Development Technical Report

ECOM-4540

AD A04C561

GROWTH AND SPECTRAL ANALYSIS OF CERIUM MAGNESIUM
ALUMINATE

R. O. Savage
G. de Lhery
T. R. AuCoin
D. W. Eckart
Electronics Technology and Devices Laboratory



October 1977

DISTRIBUTION STATEMENT

Approved for public release;
distribution unlimited.

AD No.

DDC FILE COPY

ECOM

US ARMY ELECTRONICS COMMAND FORT MONMOUTH, NEW JERSEY 07703

NOTICES

Disclaimers

The findings in this report are not to be construed as an official Department of the Army position, unless so designated by other authorized documents.

The citation of trade names and names of manufacturers in this report is not to be construed as official Government indorsement or approval of commercial products or services referenced herein.

Disposition

Destroy this report when it is no longer needed. Do not return it to the originator.

SECURITY CLASSIFICATION OF THIS PAGE (When Data Entered)

REPORT DOCUMENTATION PAGE		READ INSTRUCTIONS BEFORE COMPLETING FORM
1. REPORT NUMBER 141 ECOM-4540	2. GOVT ACCESSION NO.	3. RECIPIENT'S CATALOG NUMBER
4. TITLE (and Subtitle) 9 GROWTH AND SPECTRAL ANALYSIS OF CERIUM MAGNESIUM ALUMINATE.	5. TYPE OF REPORT & PERIOD COVERED	
7. AUTHOR(s) 10 Robert O. Savage, Jr. Thomas R. AuCoin Guy/de Lhery, Donald W. Eckart	6. PERFORMING ORG. REPORT NUMBER	
9. PERFORMING ORGANIZATION NAME AND ADDRESS Electronic Materials Research Technical Area US Army Electronics Technology & Devices Lab Fort Monmouth, NJ 07703 DRSEL-TL-E	8. CONTRACT OR GRANT NUMBER(s)	
11. CONTROLLING OFFICE NAME AND ADDRESS US Army Electronics Command DRSEL-TL-E Fort Monmouth, NJ 07703	10. PROGRAM ELEMENT, PROJECT, TASK AREA & WORK UNIT NUMBERS 16 61102A IL161102AH47 M7 011	
14. MONITORING AGENCY NAME & ADDRESS (if different from Controlling Office) 9 Research and development technical rept.	12. REPORT DATE 11 October 1977	
16. DISTRIBUTION STATEMENT (of this Report)	13. NUMBER OF PAGES 13	
15. SECURITY CLASS. (of this report) UNCLASSIFIED		
15a. DECLASSIFICATION/DOWNGRADING SCHEDULE		
17. DISTRIBUTION STATEMENT (of the abstract entered in Block 20, if different from Report) 12 16p.		
18. SUPPLEMENTARY NOTES A B C D E F		
19. KEY WORDS (Continue on reverse side if necessary and identify by block number) Ultraviolet fluorescence Energy conversion Luminescence Oxides		
20. ABSTRACT (Continue on reverse side if necessary and identify by block number) The conditions of formation from the oxides of single crystal and polycrystalline cerium magnesium aluminate have been established. The fluorescence spectra of these compounds in the near ultraviolet and the quantum efficiency of the conversion of 200-300 nm radiation have been measured. The possibility of using cerium magnesium aluminate in polycrystalline and single crystal configurations in a personal radiation detector is discussed.		

037620

13

CONTENTS

	<u>Page</u>
INTRODUCTION	1
EXPERIMENTAL	2
DISCUSSION	3
CONCLUSION	5

TABLE

1. Quantum efficiencies (q.e.) at the excitation maximum of Ce^{3+} and Ce^{3+} , Tb^{3+} -doped $\text{LaMgAl}_{11}\text{O}_{19}$. 6

FIGURES

1. Spectral energy distribution of a low-pressure pulsed xenon arc.	7
2. Spectral energy distribution of the emission of $\text{La}_{1-x}\text{Ce}_x\text{MgAl}_{11}\text{O}_{19}$.	8
3. Diffuse reflection and excitation spectra of Ce^{3+} emission in $\text{La}_{1-x}\text{Ce}_x\text{MgAl}_{11}\text{O}_{19}$.	9
4. Czochralski growth arrangement.	10
5. Electrooptical measuring system for excitation and luminescence spectra.	11
6. Excitation and luminescence spectra of ETDL $\text{CeMgAl}_{11}\text{O}_{19}$.	12
7. Energy level diagram for Ce^{3+} in YAlO_3 .	13

ACCESSION for	
NTIS	White Section
DDC	Buff Section <input type="checkbox"/>
UNMANAGED	
JUL 1 1987	
BY	
DISTRIBUTION/AVAILABILITY CODES	
Dist	1000-2000/ST SPECIAL
	

GROWTH AND SPECTRAL ANALYSIS OF CERIUM MAGNESIUM ALUMINATE

INTRODUCTION

The personal dosimeter (DT-236), a nuclear radiation detector and its associated reader (CP-696), developed by the Radiac Technical Area of the Combat Surveillance & Target Acquisition Laboratory, utilizes electromagnetic radiation in the 340-360 nanometer (nm) range during operation. This radiation (340-360 nm) causes a silver-activated, phosphate-glass dosimeter element, which is sensitive to gamma-radiation, to fluoresce in the orange-red (~ 630 nm) in proportion to the radiation damage caused in that material. Presently, a pulsed xenon flashtube is used to provide the requisite 340-360 nm radiation (Fig. 1). During operation at normal power the xenon tubes have less than the desired output in this range. In order to enhance 340-360 nm output, the tubes are pulsed under higher than normal power. When this is done, considerable enhancement in the range between 200-340 nm is also generated. This overdriving of the tube causes a reduction in useful lifetime.

Utilization of the tube output from 200-340 nm by conversion of this radiation to 340-360 nm would allow that tube to be driven at a lower power level, thus increasing its lifetime and making the operation of the detector more efficient.

The conversion of higher frequency, shorter wavelength electromagnetic radiation to lower frequency, longer wavelength radiation in atomic systems is called fluorescence. This is accomplished via the absorption of the shorter wavelength radiation by electrons in atomic orbitals within a chemical compound. These electrons are raised in energy by this absorption of radiation and after a finite period of time the electrons drop to a lower energy orbital and, in the process, radiate energy at a lower frequency and/or longer wavelength.

Recent work at N.V. Philips Laboratories, Eindhoven, The Netherlands,^{1,2} on polycrystalline cerium-containing inorganic compounds led to the consideration of $\text{La}_{1-x}\text{Ce}_x\text{MgAl}_{11}\text{O}_{19}$ as a prime candidate for the sought conversion of the electromagnetic radiation. Table 1 lists the high quantum efficiency of the conversion of 200-300 nm radiation to 340-360 nm for various stoichiometries of $\text{La}_{1-x}\text{Ce}_x\text{MgAl}_{11}\text{O}_{19}$. Figures 2 and 3 graphically demonstrate this process. The properties of the polycrystalline material may or may not reflect those of single crystal material. Discussions with Dr. A. Cohen and E. Groeber of the Radiac Technical Area resulted in the decision to investigate the possibility of forming single crystals of $\text{CeMgAl}_{11}\text{O}_{19}$ and determining its fluorescent properties.

1. J.M.P.J. Verstegen, J.L. Sommerdijk and J.G. Verriet, "Cerium and Terbium Luminescence in $\text{LaMgAl}_{11}\text{O}_{19}$," *Journal of Luminescence* 6, 425-431 (1973).

2. J.L. Sommerdijk and J.M.P.J. Verstegen, "Concentration Dependence of the Ce^{3+} and Tb^{3+} Luminescence of $\text{Ce}_{1-x}\text{Tb}_x\text{MgAl}_{11}\text{O}_{19}$," *Journal of Luminescence* 9, 415-419 (1974).

EXPERIMENTAL

Two basic techniques for the formation and growth of good quality single crystals from inorganic oxides were considered: 1) melt growth, where the crystal is grown from its own melt (congruently melting), and 2) flux growth, where the compound is dissolved in molten salts at high temperatures and, upon cooling, single crystals nucleate and grow. The first technique is preferable for there is less contamination and more perfect crystals generally result.

Polycrystalline materials are generally made from the component atomic or molecular species in the solid state (below the melting points of the components and the compound sought). Polycrystalline $\text{CeMgAl}_{11}\text{O}_{19}$ was formed by two techniques: 1) CeO_2 , MgO and Al_2O_3 were combined in stoichiometric quantities and fired at 1500°C in air, then air quenched; 2) using the approach of the Philips workers,^{3,4} MgO and $\text{Al}(\text{OH})_3$ were reacted with dilute HNO_3 forming an aqueous solution of $\text{Al}(\text{NO}_3)_3$ and $\text{Mg}(\text{NO}_3)_2$. $\text{Ce}(\text{NO}_3)_3 \cdot 6\text{H}_2\text{O}$ was added and then the hydroxides of Al , Mg and Ce were precipitated using NH_4OH . The solution was evaporated to dryness leaving a co-precipitated powder which was dried, then fired at 700°C in air for one hour. This powder was subsequently fired at 1500°C for four hours and air quenched.

The two resulting polycrystalline powders were examined by means of an x-ray powder diffractometer and were found to have the same crystal structures as $\text{CeMgAl}_{11}\text{O}_{19}$. To determine whether the compound melts congruently, the first powder was melted using an oxyhydrogen torch. The recrystallized product was shown by x-ray diffraction to be the same as the starting powder which proved the compound congruently melted.

The next step was the growth of single crystals for spectral analysis. An iridium crucible was loaded with preformed $\text{CeMgAl}_{11}\text{O}_{19}$ and raised in temperature to 2000°C in an RF generator. Here the compound was melted and then slow-cooled for purposes of nucleation and growth of single crystals. On cooling to room temperature, crystals were broken out of the crucible and used as seed crystals for the Czochralski growth method illustrated in Fig. 4. Again a melt was formed at $\sim 2000^\circ\text{C}$; a seed crystal attached to a refractory rod was lowered into the melt and then withdrawn slowly. A large single crystal grew on the seed and eventually pulled away from the melt. This crystal was removed and broken up into several large pieces with clear areas. These large pieces were examined by x-ray diffraction, and several were subjected to the following spectral analysis.

The experimental setup shown in Fig. 5 was used. Light from cw xenon lamp is filtered by two 1/4-meter Ebbert monochromators providing a tunable source with a bandwidth of 6.4 nm. This light excites the crystal to different emission intensities depending on the wavelength of the exciting light. The emission is chopped at 400 Hz to provide an ac signal for the amplifying electronics. After the emission is filtered by the 1/2-meter Ebbert monochromator at a bandwidth of 0.64 nm, it is transformed into a 400-Hz electrical signal by the RCA 7265 photomultiplier, which is cooled to -25°C to reduce shot noise. The signal is then amplified by a broadband preamplifier whose signal feeds a "lock-in" amplifier. The "lock-in" reamplifies the signal while also processing the signal by a phase sensitive detector which is driven by a 400-Hz reference signal generated at the chopper. The signal is then

3. See Reference 1, p. 1.
4. See Reference 2, p. 1.

rectified and fed to the Y channel of an X-Y recorder. The X channel is operated in the "sweep mode" calibrated to the wavelength scan speed of the appropriate monochromator.

To obtain excitation spectra the 1/2-meter monochromator is tuned to the wavelength of maximum luminescent output while the crystal is excited by the cw xenon light scanned by the 1/4-meter monochromators. Since the xenon lamp is not a gray emitter, the resultant data must be divided by the xenon spectral output to obtain a relative excitation spectrum. Replacing the sample with MgO and measuring the xenon output at the wavelength of maximum excitation by the photomultiplier via the 1/2-meter monochromator, we can compute a maximum value for the quantum efficiency q , where

$$q_{\max} = \frac{S_X(\lambda_{L\max})}{S_{Xe}(\lambda_{emax})} \cdot \frac{R_{PM}(\lambda_{emax})}{R_{PM}(\lambda_{L\max})}$$

$S_X(\lambda_{L\max})$ = emission at wavelength of maximum luminescence

$S_{Xe}(\lambda_{emax})$ = xenon signal at wavelength of maximum excitation

$\lambda_{L\max}$ = wavelength at maximum emission

λ_{emax} = wavelength at maximum excitation

R_{PM} = response of photomultiplier

Setting q_{\max} at the excitation maximum and dividing all the spectrum wavelengths by the appropriate values of the excitation wavelength, and correcting for the reflectance of the crystal, we obtain a spectrum of the quantum efficiency (Fig. 6).

To obtain luminescence or emission spectra, the 1/4-meter monochromators are tuned to the most efficient exciting wavelength, and the 1/2-meter monochromator is scanned through the appropriate wavelengths. The resultant data is divided by the spectral response of the monochromator-photomultiplier complex, yielding the luminescence spectrum (Fig. 6).

DISCUSSION

The luminescent spectra that result are based on the following: the element Ce is one of the rare-earth metals, whose 4f orbits as a group are not completely filled with electrons. In the $\text{CeMgAl}_11\text{O}_{19}$ with a close-packed oxygen anion framework, the oxygen anions which bond with the cerium atoms have filled 5s and 5p orbitals. In the Ce atoms, the 4f orbitals have 2 electrons, and in the Ce^{3+} ion of interest here, there is one 4f electron. The other 4f electron and two 6s electrons are involved in bonding the Ce^{3+} to the oxygen ligands through molecular orbitals formed by the cations' 6s and 4f orbitals and the oxygen 5s and 5p orbitals.

The single 4f electron gives rise to two energy states: the $^2F_{7/2}$ level (with quantum numbers $S=1/2$, $L=3$, $J=7/2$) and the $^2F_{5/2}$ level ($S=1/2$, $L=3$, $J=5/2$). These two levels, which differ in energy by an amount corresponding to about 2000 cm^{-1} , relate to two distinct states; in the first, the orbital and spin moments of the electron are parallel, and in the second they are anti-parallel. The 4f electron is screened from the environment by the electrons involved in the bonding orbitals.

A Ce^{3+} ion in this compound emits radiation when an electron that has been raised by excitation from a 4f to a 5d state returns to the 4f state. Unlike the 4f orbit, the 5d orbit lies at the surface of the ion and is therefore much more exposed to the influence of the crystal lattice. The electric field of the surrounding ions, the "crystal field," has the effect of splitting the 5d level into a number of sublevels (the Stark effect), which are roughly $15,000$ to $20,000 \text{ cm}^{-1}$ apart. Further, the emission and absorption bands are considerably broadened due to this interaction with the lattice.

Transitions from this level to the 4f level give rise to a band instead of discrete lines in the emission spectrum (Fig. 7). The splitting of the 4f state gives the emission a double character, i.e., the band consists of two overlapping sub-bands. The strongest emission corresponds to a transition from the lowest sublevel of the 5d level to the two 4f bands. This 5d-4f transition is a permitted transition (electric-dipole) and accounts for the very short lifetimes of the electrons in the 5d states, 30 to 100 nanoseconds in the lowest 5d level. Thus the broad luminescent peaks seen in the experimental data are due to the overlapping of two sub-bands which were broadened further by the interaction of the 5d orbitals with the lattice through the crystal field. The wavelength of the emission is due to the energy levels of the 5d levels (Fig. 7) from which the electronic transition to the 4f levels takes place.

The Philips spectra (Figs. 2 and 3) and quantum efficiencies (Table 1) were obtained using the approach of Bril and Wanmaker.⁵ They used mainly 254-nm excitation with a filter arrangement which passed only 220-296 nm radiation. In our procedure, the excitation source used is a cw xenon lamp without a filter which approximates the radiation present under the operating conditions of the dosimeter. Also, the Philips workers compared the output of the luminescent material to the luminescent output of sodium salicylate which is assumed to have a constant quantum efficiency. This was not done in this study.

Figure 6 is the experimental excitation and luminescent spectra obtained in this work and compares well with the spectra in Fig. 3. In Fig. 6, the short wavelength component (340-360 nm) of the Ce^{3+} emission of $\text{CeMgAl}_{11}\text{O}_{19}$ had a lower intensity than anticipated. We believe this is due to self-absorption of the emission by the compound itself because of the high Ce^{3+} concentration. This effect had been noted first by Botden.⁶ Based on this fact a Ce^{3+} concentration reduced by two orders of magnitude as in

5. A. Bril and W.L. Wanmaker, "Fluorescent Properties of Some Europium-Activated Phosphors," *J. Electrochem. Soc.* 111, 12 (1964).

6. P.J. Botden, "Transfer and Transport of Energy by Resonance Processes in Luminescence Solids," *Philips Res. Repts.* 7, 197 (1952).

$\text{La}_{0.99}\text{Ce}_{0.01}\text{MgAl}_{11}\text{O}_{19}$ would yield a higher luminescence output between 340 and 360 nm. Also, as Weber⁷ points out, because of the very strong absorption strength of the Ce^{3+} 5d bands, radiation at excitation or pump wavelengths penetrates only a short distance into the crystal. This implies that very thin single crystals or thin polycrystalline layers of $\text{La}_{0.99}\text{Ce}_{0.01}\text{MgAl}_{11}\text{O}_{19}$ might be the most efficient configuration, because the ratio of surface to bulk would be very high and surface luminescence should predominate.

CONCLUSION

Since it is evident that thin layers of $\text{La}_{0.99}\text{Ce}_{0.01}\text{MgAl}_{11}\text{O}_{19}$ are required for maximum conversion efficiency of 200-300 nm radiation to 340-360 nm radiation, the formation of such layers should be sought. Single crystals have been grown and characterized, and it should be possible to perfect the growth techniques to produce larger area, thin single crystals of $\text{La}_{0.99}\text{Ce}_{0.01}\text{MgAl}_{11}\text{O}_{19}$.

Other approaches consist of coating transparent substrates such as thin single crystals of Al_2O_3 (sapphire), MgAl_2O_4 (spinel), or fused quartz (amorphous) on $\text{La}_{0.99}\text{Ce}_{0.01}\text{MgAl}_{11}\text{O}_{19}$ by one of the following techniques: arc-plasma-spray, chemical vapor deposition, or liquid phase epitaxy. All of the above substrates are in our possession and the arc-plasma-spray facility is available. A testing program using the thin single crystals and/or the coated transparent substrates would then follow.

Further, since integral reflectors in xenon lamps were developed for the US Army Mobility Command by Varian Associates,⁸ one could conceive of a reflector configuration with the reflector coated with $\text{La}_{0.99}\text{Ce}_{0.01}\text{MgAl}_{11}\text{O}_{19}$. Indeed, since the xenon lamps have fused quartz envelopes, either coated quartz envelopes or envelopes of $\text{La}_{0.99}\text{Ce}_{0.01}\text{MgAl}_{11}\text{O}_{19}$ itself are other possibilities.

In summary, many physical configurations are available for use of this ultraviolet phosphor.

7. M.J. Weber, "Optical Spectra of Ce^{3+} and Ce^{3+} -Sensitized Fluorescence in YAl_5O_1 ," *J. Appl. Phys.* **44**, 3208 (1973).

8. John J. Richter, "Development of Compact Xenon Arc Lamps with Integral Reflectors," Final Report, April 1969, Contract No. DAAK02-68-C-0215, US Army Mobility Equipment Research & Development Center, Fort Belvoir, VA.

Table 1

Quantum efficiencies (q.e.) at the excitation maximum of Ce^{3+} and Ce^{3+} , Tb^{3+} -doped $\text{LaMgAl}_{11}\text{O}_{19}$.

Composition	q.e. (%)	
	Ce^{3+} emission	Tb^{3+} emission
$\text{La}_{0.99}\text{Ce}_{0.01}\text{MgAl}_{11}\text{O}_{19}$	65	--
$\text{La}_{0.90}\text{Ce}_{0.10}\text{MgAl}_{11}\text{O}_{19}$	65	--
$\text{La}_{0.75}\text{Ce}_{0.25}\text{MgAl}_{11}\text{O}_{19}$	65	--
$\text{La}_{0.50}\text{Ce}_{0.50}\text{MgAl}_{11}\text{O}_{19}$	60	--
$\text{CeMgAl}_{11}\text{O}_{19}$	60	--
$\text{Ce}_{0.9}\text{Tb}_{0.1}\text{MgAl}_{11}\text{O}_{19}$	25	35
$\text{Ce}_{0.8}\text{Tb}_{0.2}\text{MgAl}_{11}\text{O}_{19}$	10	55
$\text{Ce}_{0.7}\text{Tb}_{0.3}\text{MgAl}_{11}\text{O}_{19}$	< 5	60
$\text{Ce}_{0.65}\text{Tb}_{0.35}\text{MgAl}_{11}\text{O}_{19}$	~ 0	65
$\text{Ce}_{0.6}\text{Tb}_{0.4}\text{MgAl}_{11}\text{O}_{19}$	~ 0	60

(Reprinted from "Cerium and Terbium Luminescence in $\text{LaMgAl}_{11}\text{O}_{19}$," J.M.P.J. Verstegen, J.L. Sommerdijk and J.G. Verriet, "Journal of Luminescence 6, (1973).)

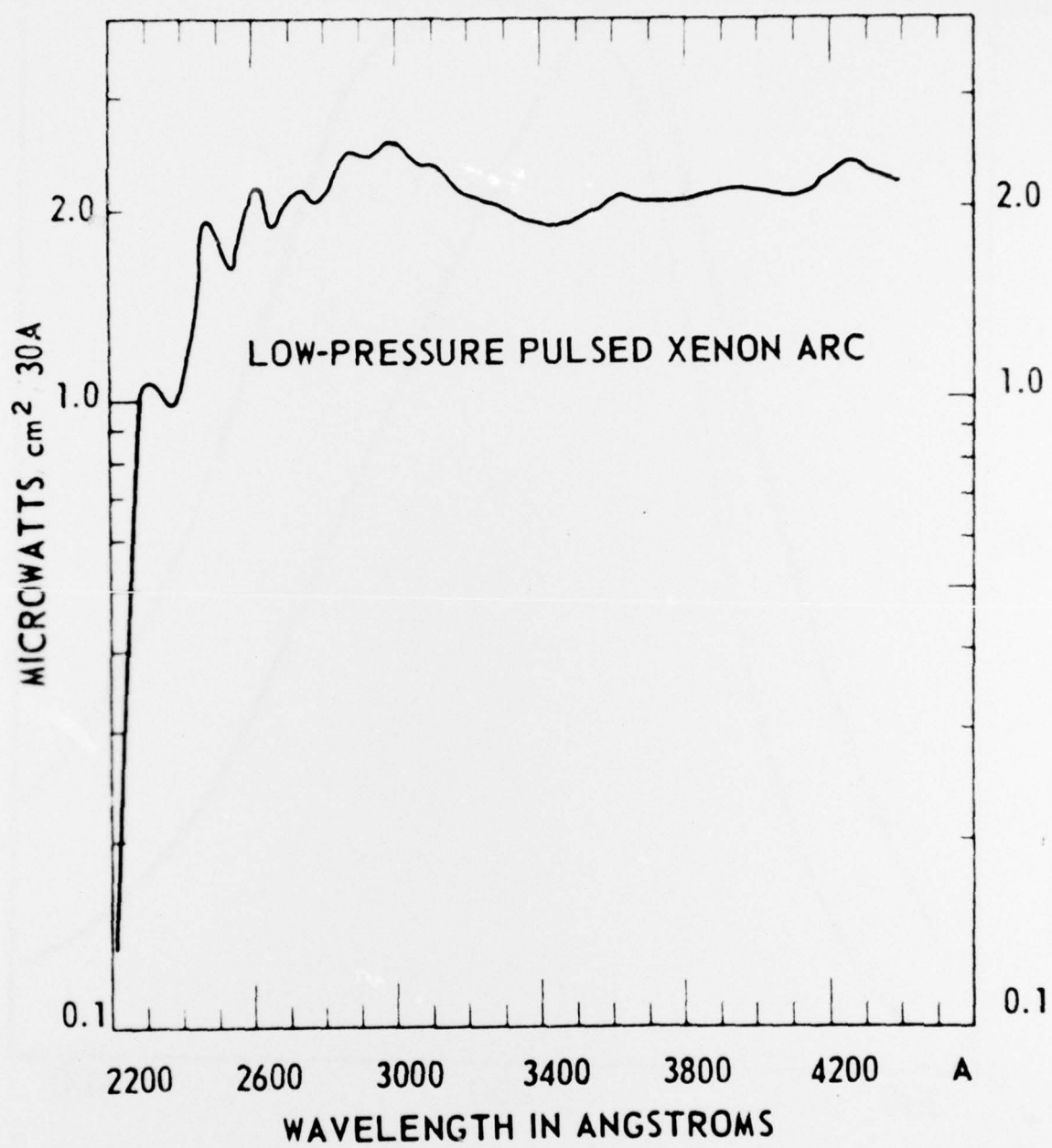


Fig. 1. Spectral energy distribution of a low-pressure pulsed xenon arc.

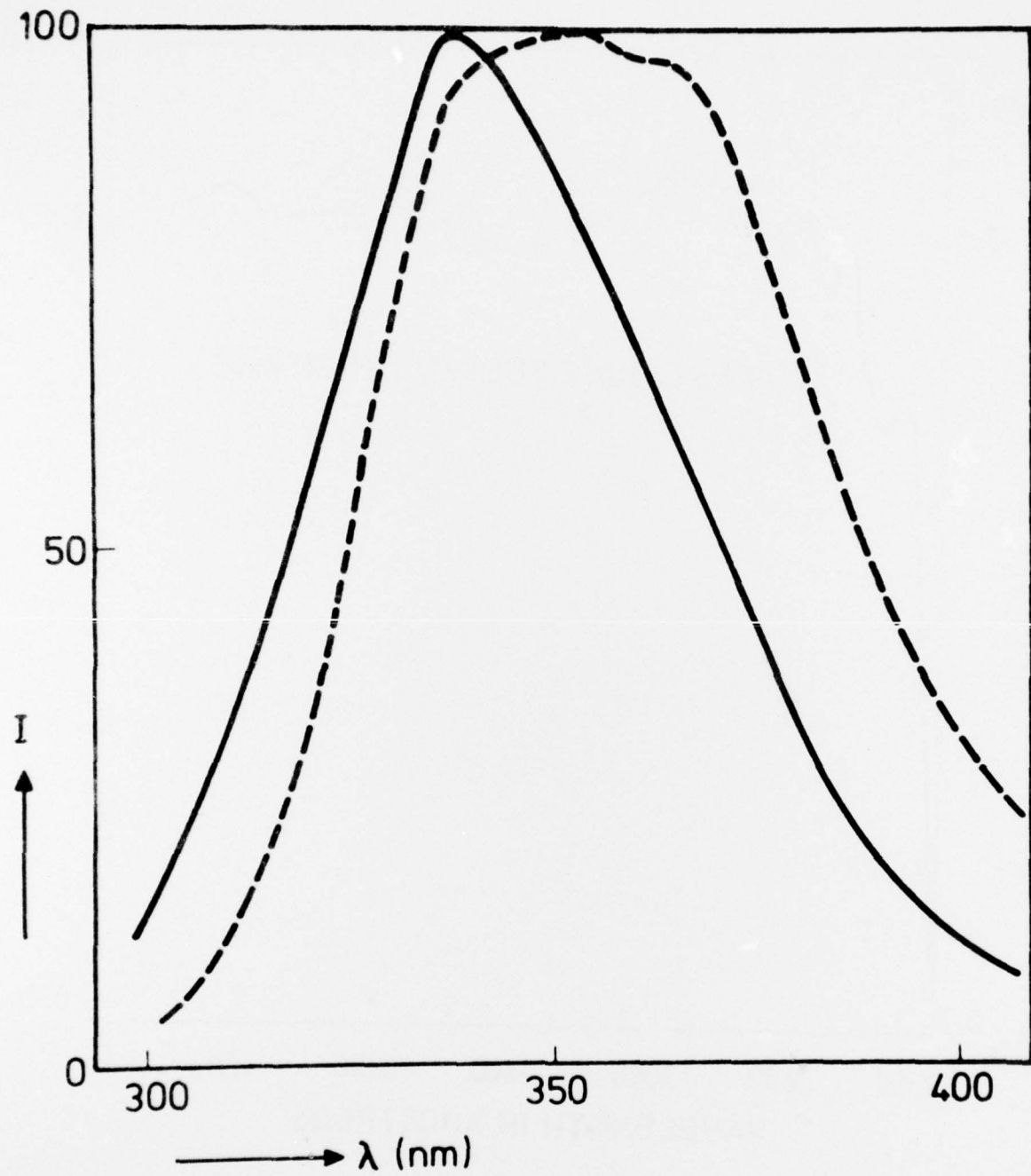


Fig. 2. Spectral energy distribution of the emission of $\text{La}_{1-x}\text{Ce}_x\text{MgAl}_{11}\text{O}_{19}$.

(Reprinted from "Cerium and Terbium Luminescence in $\text{LaMgAl}_{11}\text{O}_{19}$," J.M.P.J. Verstegen, J.L. Sommerdijk and J.G. Verriet, " Journal of Luminescence 6, (1973).)

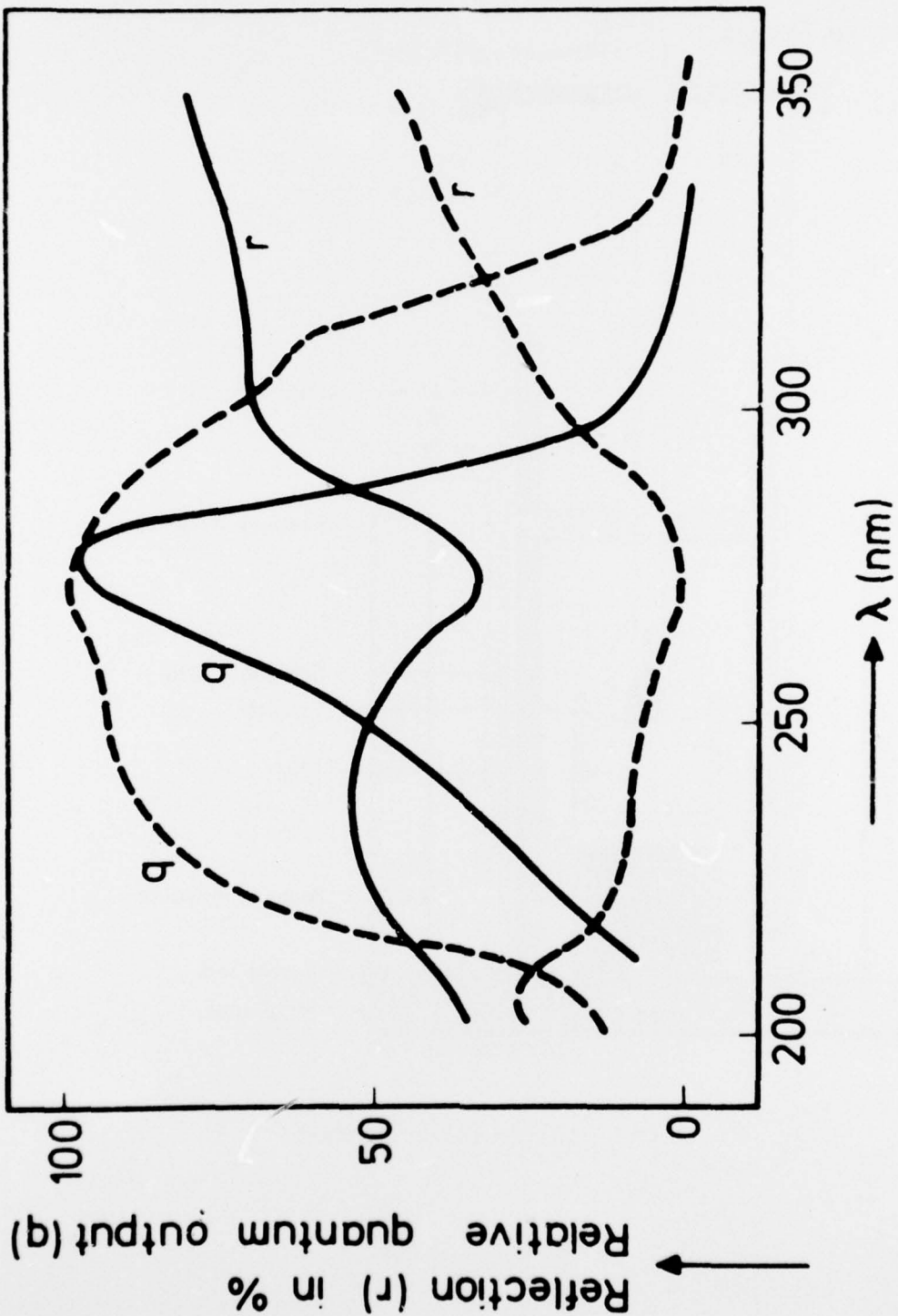


Fig. 3. Diffuse reflection and excitation spectra of Ce^{3+} emission in $\text{La}_{1-x}\text{Ce}_x\text{MgAl}_{11}\text{O}_{19}$.
 (Reprinted from "Cerium and Terbium Luminescence in $\text{LaMgAl}_{11}\text{O}_{19}$," J.M.P.J. Verstegen,
 J.L. Sommerdijk and J.G. Verrriet," Journal of Luminescence 6, (1973).)

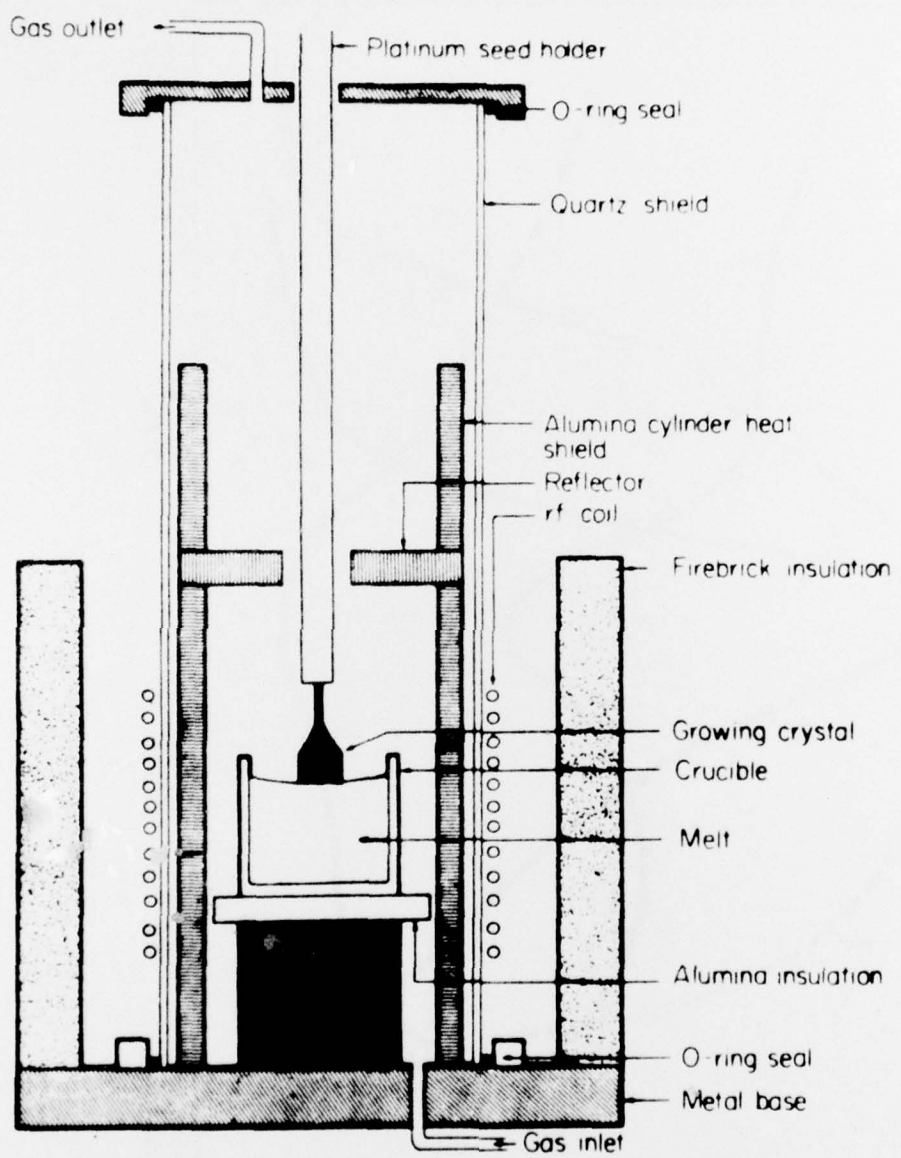


Fig. 4. Czochralski growth arrangement.

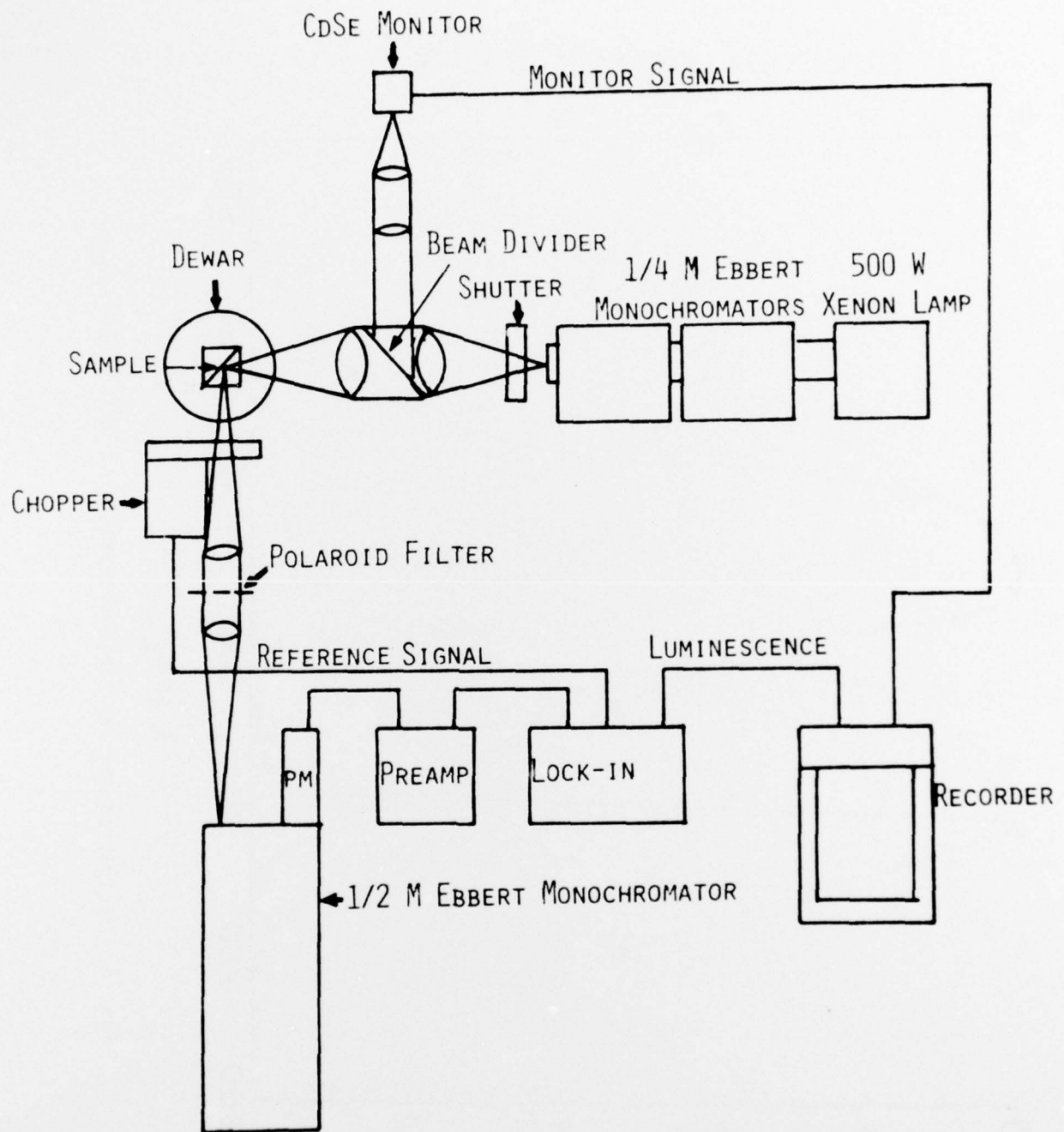


Fig. 5. Electrooptical measuring system for excitation and luminescence spectra.

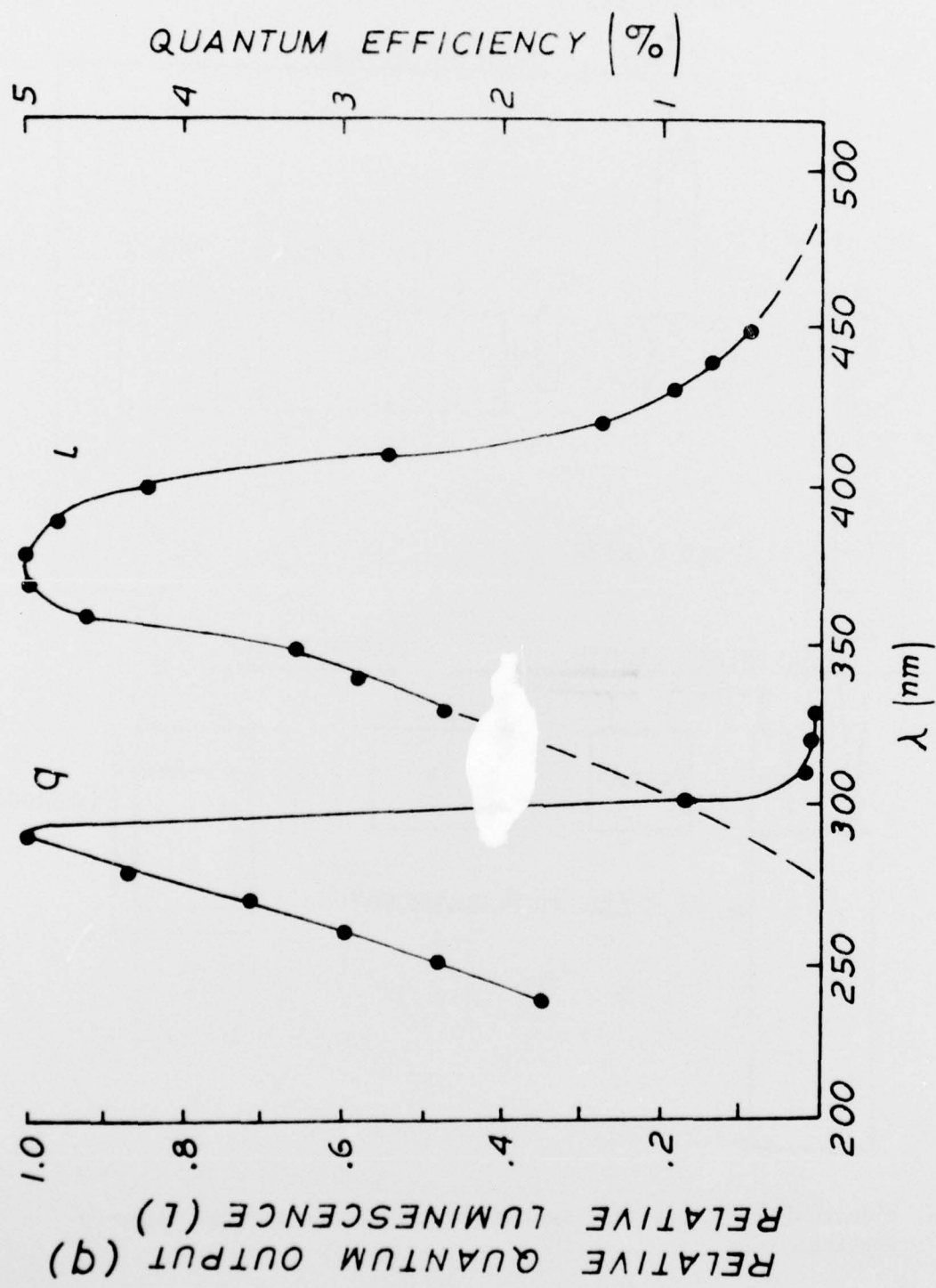


Fig. 6. Excitation and luminescence spectra of ETDL CeMgAl₁₁O₁₉.

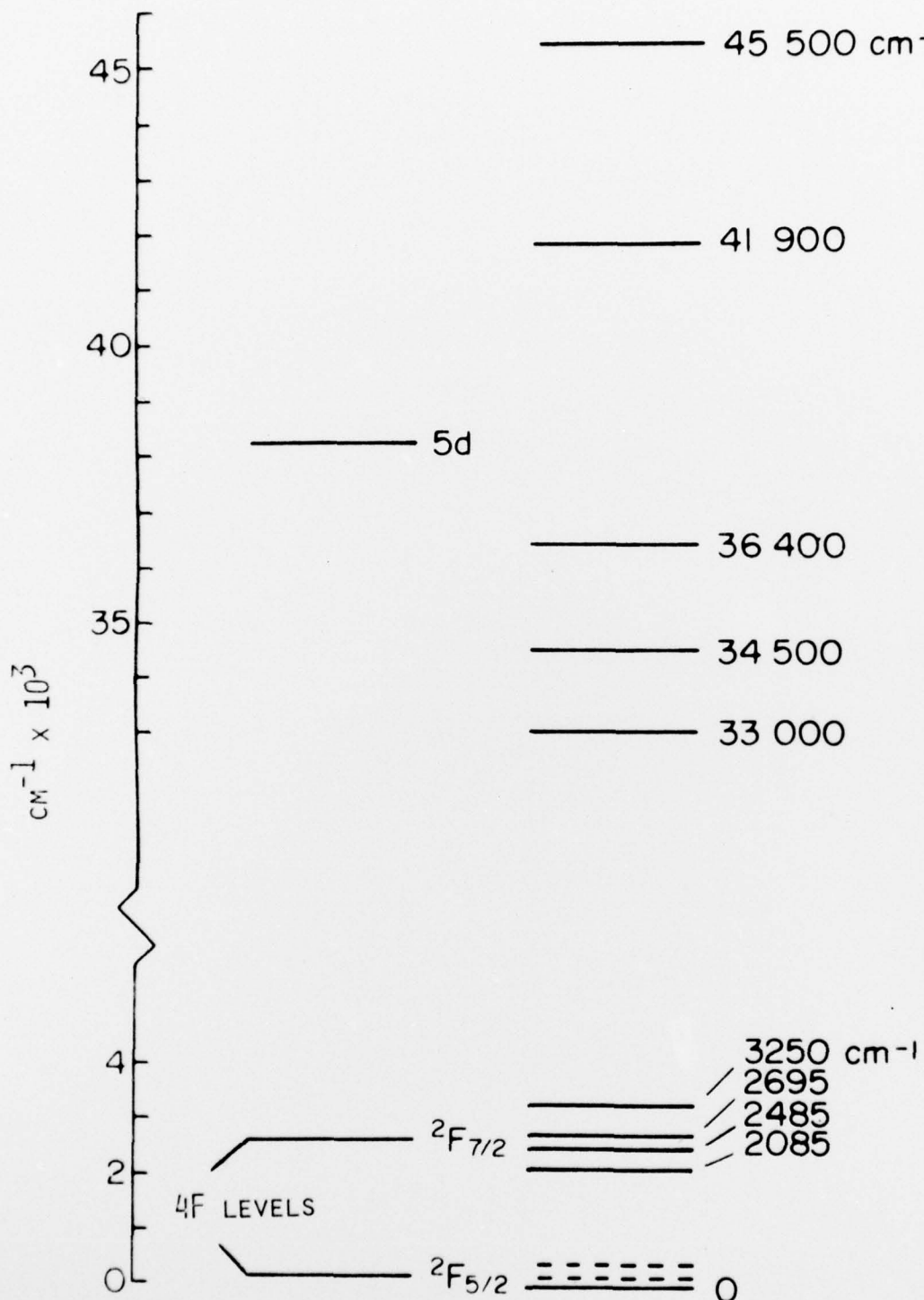


Fig. 7. Energy level diagram for Ce^{3+} in YAlO_3 .

(Reprinted from "Optical Spectra of Ce^{3+} and Ce^{3+} -Sensitized Fluorescence in YAlO_3 ," J. Appl. Phys. 44, 3208 (1973).)